




TECHNICAL ARTICLE

Study on the Effect of Liberation Properties of Phosphate Ore with Different Particle Sizes on Flotation at Different Grinding Degrees

QUAN JIANG ¹, YONG YANG,^{2,3} and LANDRY SOH TAMEHE¹

1.—China Nonferrous Metals (Guilin) Geology and Mining Co., Ltd, Guilin 541004, China. 2.—Mining College, Guizhou University, Guiyang 550025, China. 3.—e-mail: yyttmm1021@163.com

In this work, the medium-low grade calcium-magnesium phosphate ore in Zhijin, China, was investigated through systematic mineral processing studies using a scanning electron microscope, x-ray fluorescence spectrometer, and BGRIMM process mineralogy analyzer in combination with the ImageJ software and flotation experiment. The aim of this study was to suggest a process flow to optimize the flotation index of Zhijin phosphate ore. The effect of the liberation properties of fluorapatite on flotation behavior were analyzed with various particle sizes under different grinding fineness. Based on the characteristics of fluorapatite, we propose a double reverse flotation process with two routes for coarse- and fine-grained ore, respectively. The results showed that the flotation process can effectively improve the grade of phosphate ore and reduce the MgO content. As the degree of liberation increases, the flotation index increases first, and when the liberation degree reaches a certain value, the flotation index decreases. The maximum grade of fluorapatite was obtained for a grinding fineness of 82.86%, while the maximum grade of P_2O_5 was obtained for the $-53 + 38\text{-}\mu\text{m}$ particle size for flotation concentrate at various particle sizes.

INTRODUCTION

Guizhou Province in China hosts large-scale phosphate ore deposits rich in rare earth ores; however, exploitation of this resource over time has led to a depletion of reserves of high-grade phosphate ore. In addition, due to the difficulty of studying phosphate and rare earth ore resources separately, rare earth phosphate ore is still under-exploited in the central part of Guizhou, especially in the Zhijin area.¹ In this area, the phosphate mineral is mostly fluorapatite, while dolomite is the main gangue mineral. Due to the complicated co-existence between fluorapatite and dolomite, it is very difficult to separate the two minerals. Froth flotation is presently the most effective method for separating dolomite from phosphate ore.^{2,3} Before flotation, phosphate ore is crushed and ground to

achieve complete liberation of minerals, which plays a critical role in flotation.^{4,5} To address the issue in separating dolomite from fluorapatite at Zhijin, systematic process mineralogy research has been proven to provide the best processing flowsheet based on a comprehensive understanding of the mineral components of phosphate ore; therefore, for the research of process mineralogy, the development of testing instruments plays an extremely important role.

The polarizing microscope, developed in the late nineteenth century,^{6,7} has had important applications in engineering disciplines such as geology and process mineralogy. This microscope is a reliable piece of equipment for the observation and analysis of minerals under three observation modes including single-polarized, cone, and orthogonal polarized light. Based on the poor light transmittance of fluorapatite under single-polarized light, Yang et al.⁸ measured the liberation degree of fluorapatite under different grinding fineness, while Guo et al.⁹

(Received August 22, 2023; accepted January 29, 2024; published online March 14, 2024)

determined the liberation degree of fluorapatite at different particle sizes by using a BX51-P polarizing microscope.

With the development of new and updated technologies, process mineralogy studies have changed from the application of a traditional polarizing microscope to the scanning electron microscope (SEM), with upgraded resolution from 25 nm to 0.01 nm. This offers the possibility to use SEM in conjunction with an energy-dispersive spectrometer (EDS) to generate high-resolution backscattered secondary electron (BSE) images, which are useful to characterize the shape, structure, and size of minerals.^{10–13} The emergence of the MLA (mineral liberation analyzer) system, combined with the advantages of SEM-EDS,^{14–16} offers valuable optimized solutions for automated quantitative mineral characterization.^{17,18} Hence, the advanced SEM-based MLA technique provides accurate and targeted automated mineral information such as the composition, particle size, liberation, and theoretical maximum recovery of the minerals.^{19–21} Based on this technique, Xu et al.¹⁸ have quantitatively determined the degree of liberation and particle size of useful minerals of sphalerite tailings, which are required to predict the effective recovery of these minerals in the tailings and guide the subsequent separation process.

Furthermore, the MLA has been applied in numerous studies to document the effect of mineral liberation on the flotation of different minerals. Xiao et al.²² performed vertical stirred mill and ball mill grinding tests for magnetite, with the distribution of particle size and liberation degree of minerals tested by MLA. The results indicate that stirred milling significantly increases the liberation degree of magnetite 8.1% more than ball milling, and the iron grade of the magnetic separation concentrate of stirred milling is 5.2% times higher than that of the ball milling.

Abdollahi et al.²³ conducted process mineralogy studies by MLA on the feed, concentrate, and tailings of molybdenite to determine the degree of liberation of useful minerals in the molybdenum concentrate. These authors found that there was a complicated co-existence between pyrite and chalcopyrite. The low liberation degree of the useful mineral in the feed was the reason for the low iron and copper content in the molybdenum concentrate.

In recent years, automated mineral information has been further obtained using BPMA (BGRIMM process mineralogy analyzer),²⁴ which is a modern and reliable technology equipped with the SEM-EDS system that makes automatic mineral analysis more convenient and accurate.^{25,26} The BPMA is cutting-edge technology and an effective technique that allows achieving fast and complete automated quantitative measurements of the composition, distribution, liberation degree, particle size distribution, occurrence state, and other parameters of minerals. For example, Wen et al.²⁷ applied BPMA

to extract mineralogical information of raw coals such as the composition, liberation degree, and interlocking parameters of useful minerals and gangue, providing technical references for fine processing of coal resources.

The present work focuses on Zhijin phosphate ore and investigates the effects of liberation properties of fluorapatite with various particle sizes under different grinding fineness conditions and flotation behavior. The study aims to optimize the flotation index of Zhijin phosphate ore, which is crucial to enhance the processing of medium-low grade ore to achieve sustainable development for the phosphate ore industry in China.

EXPERIMENTAL SECTION

Sample Preparation

The ore samples (60 kg) were collected from the Zhijin area in Guizhou Province, Southwest China. The ore consists of alternating black and gray layers, with thickness ranging from 1.5 cm to 2 cm and from 6 to 8 cm, respectively. First, the ore was crushed to – 1 mm particle size using a jaw crusher (model SP100 × 6, Guiyang Prospecting Machinery Factory, Guiyang, China), then taking an appropriate amount of – 1mm sample to making polished sections with 30 mm diameter using epoxy resin. The polished sections were then subjected to rough grinding, fine grinding, ultra-fine grinding, and polishing treatment. The treated polished sections were naturally dried following an ultrasonic decontaminated treatment and finally coated with carbon spray to enable the sections to conduct electricity; polished sections were prepared for BPMA analyses. A small portion of the – 1 mm sample was ground to – 74 μm using a conical ball mill (model XMQ-240 × 90 Wuhan Prospecting Machinery Factory, Wuhan, China) for x-ray fluorescence spectrometer (XRF) detection.

In addition, some samples were ground with a conical ball mill with 200 g of grinding feed at a time and 60% slurry concentration, and five batches of grinding experiments were carried out for 3 min, 4 min, 5 min, 6 min, and 7 min, respectively. The grinding products were then wet-sieved with – 0.074 mm sieve to obtain feed products with different percentages of grinding fineness including 59.75%, 69.11%, 82.86%, 92.31, and 95.02%. All the feed products were used for the flotation experiments.

Flotation Experiment

The sample (200 g) was put into a single-cell flotation machine (model XFDIV0.75, Jilin Prospecting Machinery Factory, Jilin, China). Water was added to the pulp mass fraction of 30%. The flotation machine speed and pulp temperature were set at 1800 r/min and 20 °C, respectively. Flotation experiments were performed using a

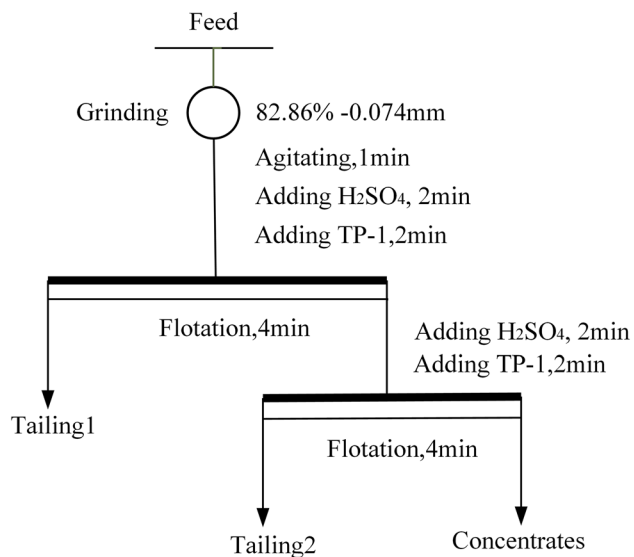


Fig. 1. Flowsheet for flotation experiment.

double reverse flotation, with the reagent sulfuric acid (H_2SO_4) used as a pH regulator for removing silicate minerals and TP-1 used as a magnesium removal collector. Analytical tests were carried out to investigate the effects of milling fineness, pH, and dosage of reagent H_2SO_4 and TP-1 on the flotation index. The flowsheet of the flotation experiment is shown in Fig. 1.

Chemical Analyses

The chemical compositions of phosphate ore samples were determined by XRF analyses using a Panalytical Zetium instrument (The Netherlands), and the results indicate medium-low grade phosphate ore, with P_2O_5 , MgO, and SiO_2 contents of 20.03%, 12.5%, and 3.45%, respectively.

Mineral Analyses

The mineral processing analysis of the crushed raw ore of -1 mm was carried out by means of BPMA at the University of Science and Technology, Beijing, China. The carbon-sprayed polished sections were loaded onto the sample chamber, with the possibility of introducing nine sections at one time. The BPMA and SEM parameters were adjusted, with an acceleration voltage set to 20 kV and a working distance set to 15.11 mm. The SEM was continuously measured in the high vacuum state of the sample chamber. The measurement method was backscatter mode. The magnification was adjusted according to the actual observation needs. The analysis was finally completed in the full particle measurement mode of the system.

Degree of Liberation Studies

SEM (model TESCAN) has been used to determine the degree of liberation as well as the association of fluorapatite and gangue minerals in feed and concentrate of flotation circuit. First, each sample of feed and concentrate was wet-sieved into four particle sizes ($-106 + 75 \mu m$, $-75 + 53 \mu m$, $-53 + 38 \mu m$, and $-38 + 25 \mu m$). Seven particle sizes ($-200 + 150 \mu m$, $-150 + 125 \mu m$, $-125 + 106 \mu m$, $-106 + 75 \mu m$, $-75 + 53 \mu m$, $-53 + 38 \mu m$, and $-38 + 25 \mu m$) were also obtained after grinding for 3 min products, and then these samples were prepared into polished sections with 30-mm diameter, and a total of 46 samples were made. Each polished section was studied using a magnification of $200-300 \times$ and a voltage set to 20 kV. Ten to 12 BSE images were taken for each sample, with each picture having about 250 particles, and each sample had a total of about 2500–3000 particles.

The BSE images were analyzed using ImageJ software to determine the mineral liberation degree and association. A grid pattern was mapped on each of the corresponding images. Processing tools of the software such as denoising, filtering, and binarization were repeatedly operated on these images to meet the expectations. Then, with the count tool, the point count of the liberated and locked mineral grains were determined. Finally, all the data were transferred to Excel, and the calculations related to the average degree of liberation of fluorapatite for different images were conducted.

Notably, mineral liberation assessment of particles commonly involves two-dimensional (2D) measurements of particle cross-section, which can be studied in 2D using the Voronoi model of Takao Ueda et al.,²⁸⁻³¹ which measures the 3D liberation based on 2D studies.

RESULTS AND DISCUSSION

Flotation Products at Different Particle Sizes

The results show that the main phosphorus-bearing ore minerals in the flotation feed are fluorapatite (57.62%), dolomite (25.34%), quartz (8.72%), calcite (5.45%), and pyrite (0.53%), while the main gangue minerals are dolomite by BPMA analysis.

The particle size of the main minerals is shown in Fig. 2. The cumulative distribution of $-74 \mu m$ and $-38 \mu m$ fluorapatite is 29.93% and 11.15%, respectively. The cumulative distribution of $-74 \mu m$ and $-38 \mu m$ dolomite is 36.17% and 12.94%, respectively, and the cumulative distribution of $-74 \mu m$ and $-38 \mu m$ quartz is 59.36% and 39.74%, respectively. The cumulative distribution rate of $-74 \mu m$ quartz is 59.36%, and that of $-38 \mu m$ quartz is 39.74%. The average particle size of fluorapatite is

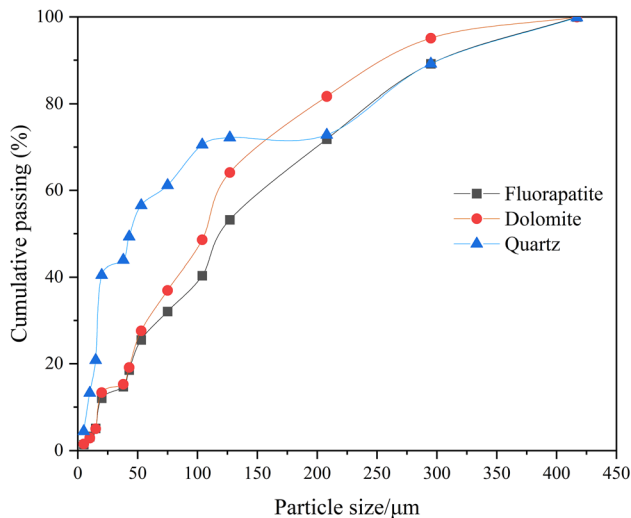


Fig. 2. Cumulative particle size distribution of major minerals.

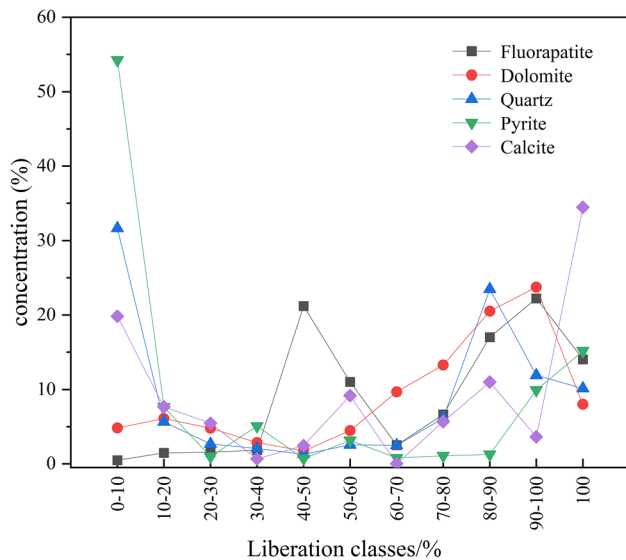


Fig. 3. Liberation classes of minerals from the phosphate ore.

160.8 μm , dolomite is 136.1 μm , and quartz is 111.5 μm . Fluorapatite is the largest mineral, followed by dolomite and quartz. The difference between the average particle sizes of dolomite and quartz is relatively small (Fig. 2).

The liberation classes of minerals from the phosphate ore are given in Fig. 3. The liberation of fluorapatite in -1 mm raw ore is low, with 14.05% of completely liberated single particles. A liberation degree of 90–100% corresponds to 22.22%, while that of 40–60% is 33.21%, with the presence of more unliberated particles. The single particles of dolomite, quartz, pyrite, and calcite are 8.01%, 10.15%, 15.16%, and 34.46%, respectively. The BPMA analysis reveals that it is difficult to separate fluorapatite from the gangue minerals by crushing the phosphate ore, while there are also many mineral associations in the phosphate ore. Therefore, it is

necessary to continue using ball milling to separate these minerals.

When the fineness of grinding is -0.074 mm with a proportion of 82.86%, the dosage of H_2SO_4 and TP-1 reaches 12 kg/ton and 1000 g/ton, respectively. As a result, the P_2O_5 content in the phosphate concentrate is 32.4%, while that of MgO is 1.6%, and the recovery of the concentrate is 86.28%.

The sieve analysis of the concentrate was carried out to investigate the distribution of P_2O_5 and MgO in the concentrate for each grain size and then to analyze the P_2O_5 content and the removal effect of MgO for each grain size. The sieve analysis results are shown in Table I.

Table I shows that P_2O_5 is abundant in $-53 + 38$ μm particle of the concentrate. The P_2O_5 content of 33.43% for this particle is the highest and the MgO recovery is the lowest amongst all particles. This result indicates that the separation is better achieved at this particle size.

Table II shows that the recovery of P_2O_5 and MgO of the tailings increases with the decrease of particle size. When the particle size is < 25 μm , the recovery of P_2O_5 and MgO is 17.23% and 50.33%, respectively. This indicates that the removal of P_2O_5 and MgO occurs in < 25 μm particle of the concentrate. Therefore, it is suitable to separate > 25 μm particle to avoid the loss of phosphate ore.

MINERALOGICAL STUDY OF FLOTATION FEED

Fluorapatite is the valuable mineral in the flotation feed, as depicted in Fig. 4. In addition to banded and rounded apatite, there is also irregular granular apatite. The size of apatite predominantly ranges from 20 to 120 μm , with some < 20 μm particles. Apatite coexists with dolomite and quartz, and it is surrounded by pyrite and calcite. Dolomite typically appears as irregular rounded, granular, or massive grains of 20 and 60 μm in size, while some particles are 60–100 μm . Calcite is commonly found at the edges of apatite and dolomite, with a grain size ranging from about 10 to 30 μm . Pyrite occurs as 5 to 20 μm grain often embedded around apatite.

ANALYSIS OF LIBERATION CHARACTERISTICS AT DIFFERENT GRINDING FINENESS

Figure 5 indicates that the liberation of fluorapatite, dolomite, and quartz increases with the increase of the grinding fineness. The best ore liberation was achieved at a grinding fineness of 82.86%, the fluorapatite-dolomite association content is low, but the liberation of fluorapatite is only obtained at 62.12%. Therefore, the Zhijin phosphate ore is difficult to liberate and belongs to the fine-grained refractory ore.

Figure 6 indicates that the grade of phosphorus concentrate increases and then decreases with the increase of the liberation degree of fluorapatite.

Table I. Analysis of P₂O₅ and MgO in concentrates with different grain sizes (%)

Particle size / μm	Productivity	P ₂ O ₅ grade	P ₂ O ₅ recovery	MgO grade	MgO recovery
- 106 + 75	23.30	27.32	31.78	6.56	12.22
- 75 + 53	16.33	28.87	23.53	2.84	3.71
- 53 + 38	14.56	33.43	24.30	1.93	2.24
- 38 + 25	14.86	28.63	21.24	0.97	1.15
0-25	31.25	27.53	42.95	1.58	3.95

Table II. Analysis of P₂O₅ and MgO of different particle sizes in tailings (%)

Particle size / μm	Productivity	P ₂ O ₅ grade	P ₂ O ₅ recovery	MgO grade	MgO recovery
- 106 + 75	6.60	9.36	3.08	9.56	5.04
- 75 + 53	5.45	11.56	3.14	11.96	5.21
- 53 + 38	10.36	6.54	3.38	12.52	10.37
- 38 + 25	22.35	5.36	5.98	14.56	26.03
0-25	55.24	6.25	17.23	11.39	50.33

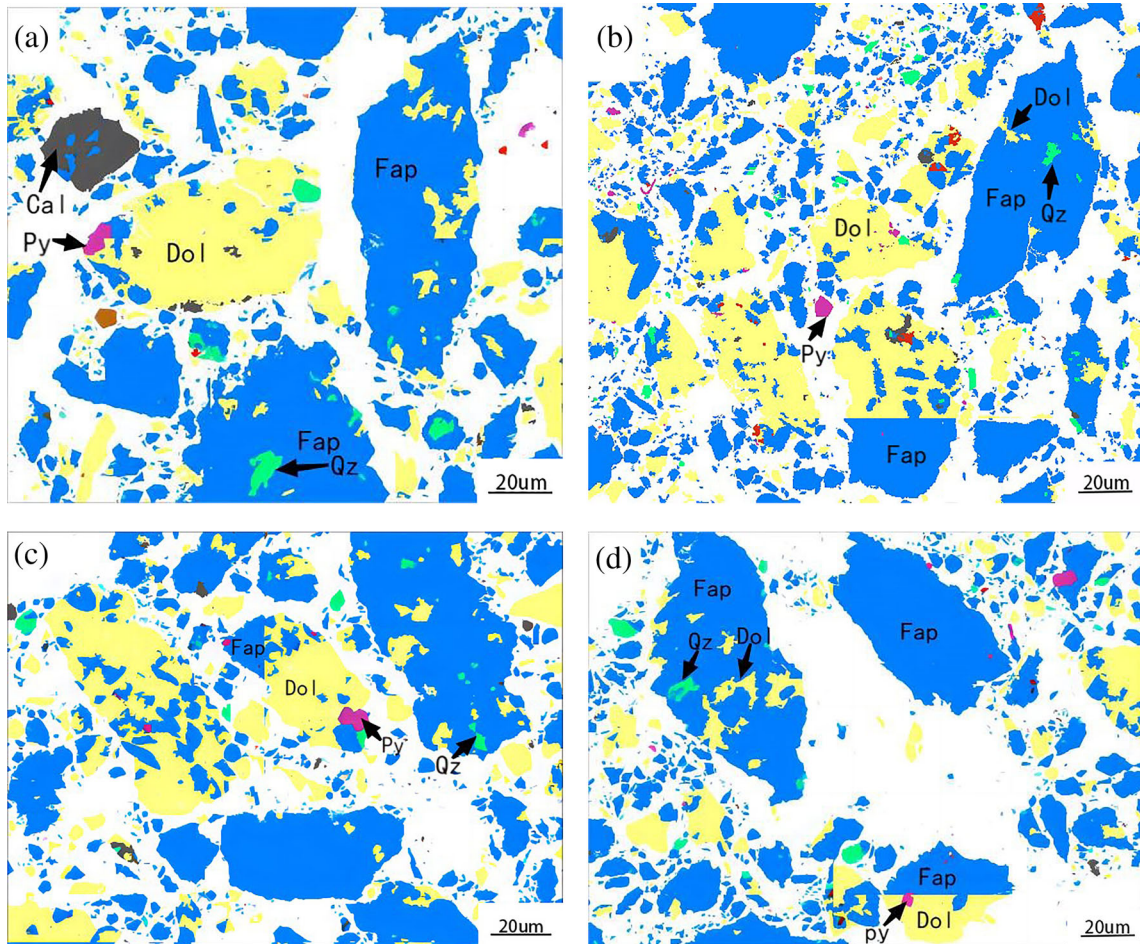


Fig. 4. BSE images of the main minerals from BPMA (Fap: fluorapatite, Dol: dolomite, Qz: quartz, Cal: calcite, Py: pyrite).

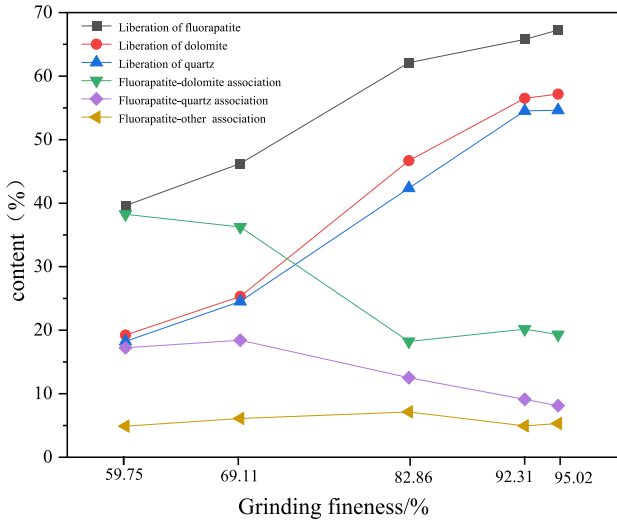


Fig. 5. Content of individual mineral and mineral associations under different grinding fineness.

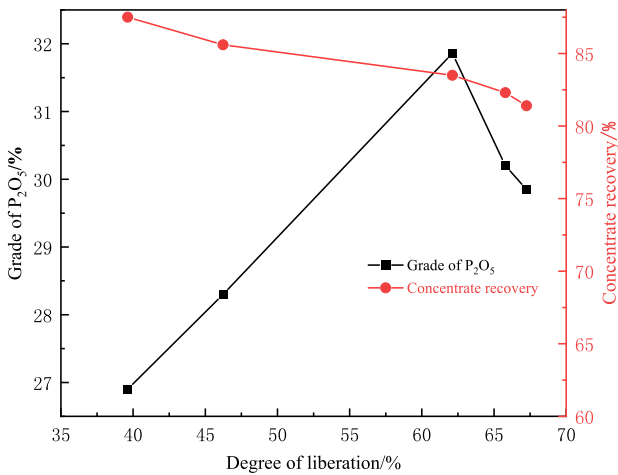


Fig. 6. Influence of liberation degree on flotation index under different grinding fineness.

When the liberation degree is 62.12%, the highest grade is 31.86%, but the recovery of phosphate concentrate decreases with the increase of liberation degree; results are shown in Fig. 6.

Notably, the liberation degree is not higher, and the flotation index is better, when the degree of liberation increases to a certain extent; the fine mineral particles increase in the ore, and the bubble properties will change. This results in a stronger entrainment effect on fluorapatite, which causes a significant loss of fluorapatite in the concentrate, so the concentrate grade decreases.

LIBERATION PROPERTIES OF FLUORAPATITE AT DIFFERENT PARTICLE SIZES

The useful mineral in the flotation feed is fluorapatite. To gain a deeper understanding of the relationship between fluorapatite and other

minerals, the above studies have shown that the flotation index is optimal when the grinding fineness is 82.86%. Therefore, under this grinding fineness, the liberation properties of minerals in the raw ore and concentrate were analyzed.

In Fig. 7, the content of fluorapatite-dolomite in the raw ore is relatively high and the degree of liberation is low. In the concentrate, the degree of liberation of fluorapatite is 80.19%, with a high liberation. However, there is also a small amount of fluorapatite associated with gangue minerals.

Figure 8 indicates that the separation effect is good, and the liberation degree of various particle sizes of fluorapatite is greatly improved after flotation. The best degree of liberation of fluorapatite is obtained for the $-38 + 25\text{-}\mu\text{m}$ particle. There is more association between fluorapatite and gangue minerals in the raw ore for the $+53\text{-}\mu\text{m}$ particle.

The content of fluorapatite in the whole concentrate increases significantly, ranging from 62.12% to 80.19%, compared to that of the raw ore, while the content of fluorapatite-dolomite decreases from 18.13% to 12.00%. It indicates that the collector has a good adsorption effect on dolomite, with more selection of dolomite though there is more association with this mineral in the concentrate. It is necessary to further optimize the grinding fineness or the dosage of flotation chemicals.

ANALYSIS OF THE EFFECT OF LIBERATION ON FLOTATION

Figure 9 shows that the degree of liberation of the raw ore and concentrate increases with the decrease of the particle size of minerals. Furthermore, the grade of the raw ore and concentrate first increases and then decreases with the increase of the degree of mineral liberation, while the recovery of the concentrate is still decreasing. It shows that within a certain range, the degree of liberation of mineral increases, which can improve its flotation index. When it increases to a certain extent, the mineral appears to be sliming, with many fine particles, which enhances the entrainment effect on fluorapatite, leading to a decrease in grade and loss of phosphate ore. Therefore, it is important to control the grinding fineness reasonably.

In Fig. 10a, the degree of liberation can reach $>90\%$ when the particle size of a mineral is coarse. The trend of the degree of liberation increases slowly with the decrease of the mineral particle size. The highest grade of P_2O_5 is observed for the $-53 + 38\text{-}\mu\text{m}$ particle.

In Fig. 10b, the liberation degree of fluorapatite in the raw ore and concentrate increases with the increase of grinding fineness. The P_2O_5 grade of concentrate first increases and then decreases, while the concentrate recovery first increases, then decreases, and finally increases. The highest P_2O_5 grade of concentrate is observed for the $-53 + 38\text{-}\mu\text{m}$ particle when the fineness of grinding is 82.86%,

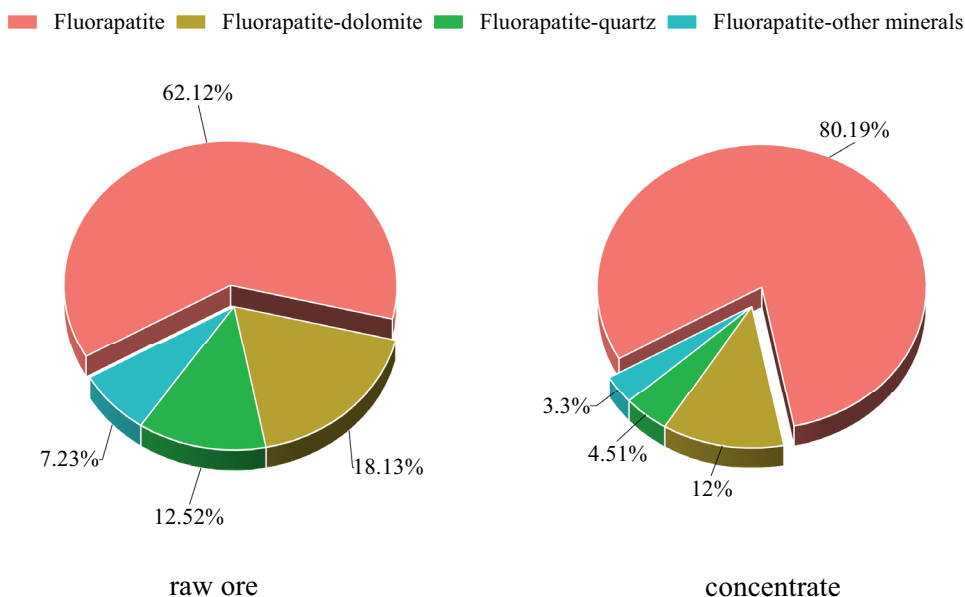


Fig. 7. Liberation statistics of fluorapatite in raw ore and concentrate.

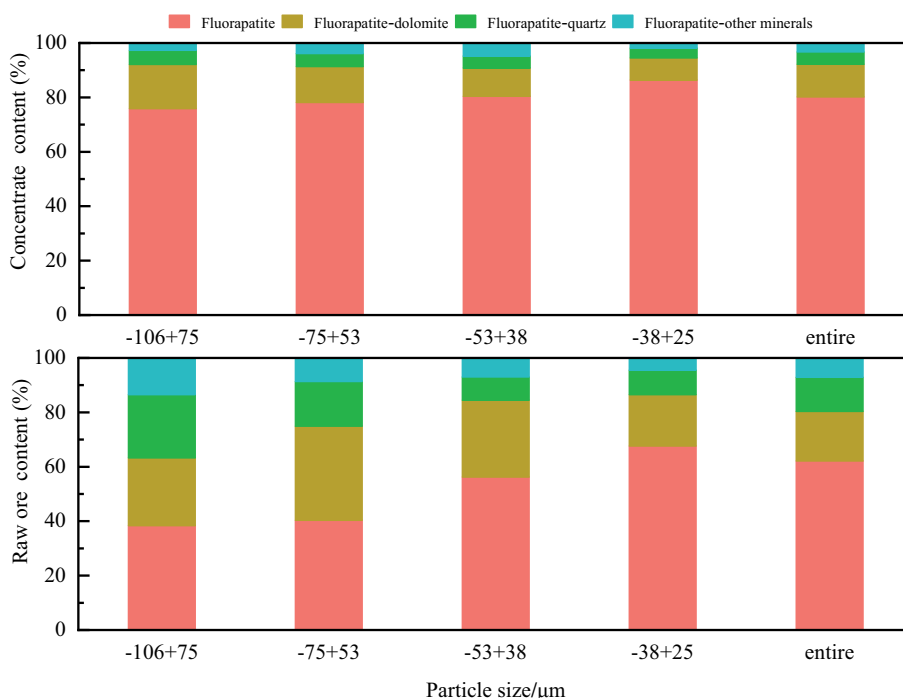


Fig. 8. Statistics of fluorapatite and association in different particle sizes of raw ore and concentrate.

and the recovery of concentrate is the best at this particle size. In summary, the flotation index of this particle size is the best. It is recommended to appropriately increase the grinding fineness to improve the yield of minerals in the $-53 + 38 \mu\text{m}$ particle, but it should be noted that grinding should not cause over-grinding to avoid sliming, thereby reducing the flotation index.

CONCLUSION

The research content has important guiding significance for the optimization of phosphate ore beneficiation technology in this area. The main conclusions are as follows:

- (1) Useful mineral of the ore is fluorapatite, while the gangue minerals are dolomite and quartz. Fluorapatite is mainly associated with dolo-

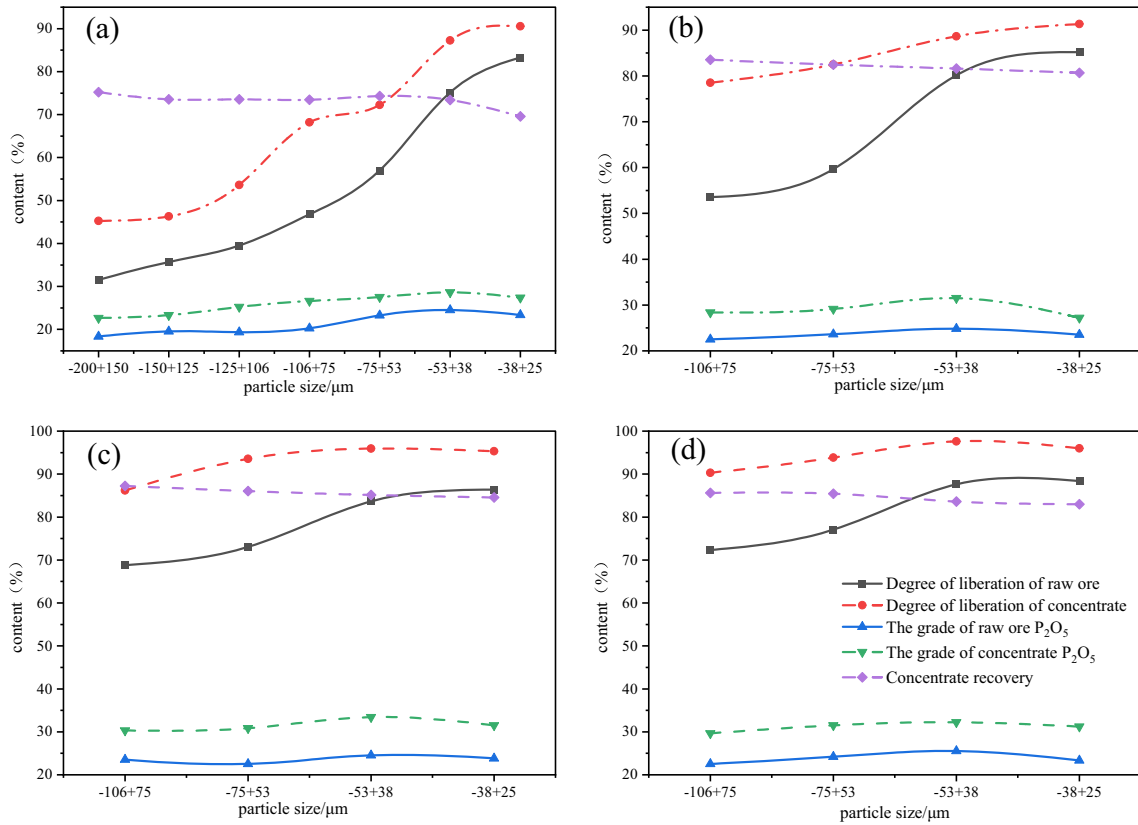


Fig. 9. Influence of the liberation degree of each particle size on flotation behavior at different grinding degrees: (a) 59.75%, (b) 69.23%, (c) 82.26%, (d) 92.31%.

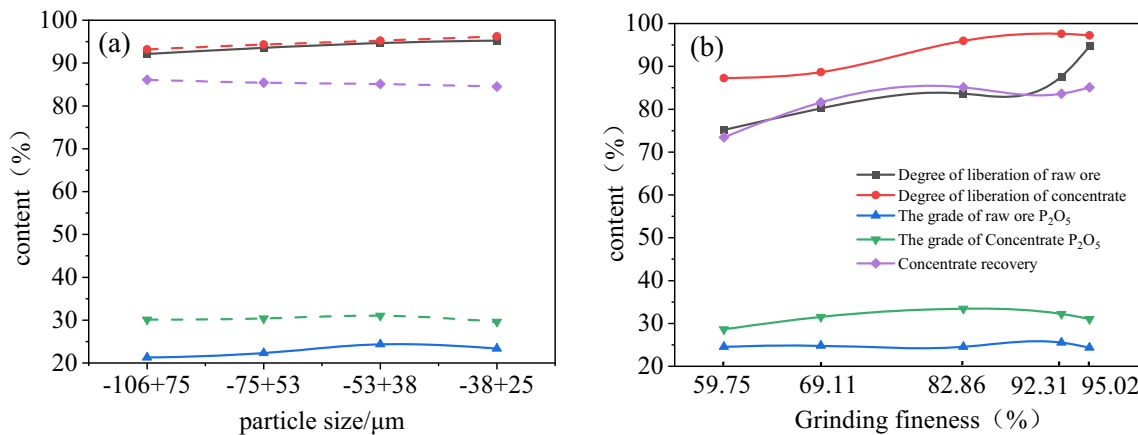


Fig. 10. Influence of liberation degree of each size on flotation behavior: (a) grinding fineness is 95.02%; (b) - 53 + 38 μm for each grinding fineness.

- (2) The degree of liberation for mineral increases with the increase of grinding fineness. The best flotation index is obtained when the liberation degree is 62.12%.
- (3) The grade of fluorapatite increases with the increase of liberation degree, and when it reaches a certain value, the grade begins to decrease; therefore, it is not the higher degree

- of liberation, the better the flotation index.
- (4) The best mineral flotation index is obtained for - 53 + 38 μm particles when the grinding fineness is 82.86%.

ACKNOWLEDGEMENTS

This study was supported by the Science and Technology Fund of Guizhou Province (QKHJZ-2011-2326, GDJHZ-2010-007), Guizhou Province Science and Education Young Talents Cultivation

Project (GPSCZ-2012-153) and Guangxi Key Research and Development Project (GK-AB21076013).

CONFLICT OF INTEREST

The authors state that there is no conflict of interest.

REFERENCES

1. Q. Jiang, Y. Yang, Y. Tang, and H. Piao, *Mineral. J.* 43, 358 (2023).
2. J. Li, G. Nie, J. Li, Z. Zhu, and Z. Wang, *Colloids Surf. A Physichem. Eng. Asp.* 641, 128586 <https://doi.org/10.1016/j.colsurfa.2022.128586> (2022).
3. W. Li, Z. Huang, H. Wang, R. Liu, L. Ouyang, S. Shuai, S. Zhang, C. Cheng, X. Yu, G. He, et al., *Sep. Purif. Technol.* 307, 122817 <https://doi.org/10.1016/j.seppur.2022.122817> (2023).
4. J. Chen, L. Lan, and X. Liao, *Trans. Nonferrous Met. Soc. China* 23, 824 [https://doi.org/10.1016/S1003-6326\(13\)62535-2](https://doi.org/10.1016/S1003-6326(13)62535-2) (2013).
5. N.O. Lotter, D.L. Kowal, M.A. Tuzun, P.J. Whittaker, and L. Kormos, *Miner. Eng.* 16, 857 [https://doi.org/10.1016/S0892-6875\(03\)00207-3](https://doi.org/10.1016/S0892-6875(03)00207-3) (2003).
6. M. Yoshikawa, and T. Toda, *J. Eur. Ceram. Soc.* 24, 521 [https://doi.org/10.1016/S0955-2219\(03\)00196-1](https://doi.org/10.1016/S0955-2219(03)00196-1) (2004).
7. T. Chunyan, D. Haojie, T. Shuo, J. Liuyun, M. Bingli, W. Yue, Z. Na, S. Liping, and S. Shengpei, *Int. J. Biol. Macromol.* 160, 142 <https://doi.org/10.1016/j.ijbiomac.2020.05.142> (2020).
8. W.Q. Yang, S.X. Fang, and J.T. Pang, *J. Wuhan Eng. Univ.* 36, 31 (2014).
9. Y.J. Guo, L.P. Du, P.Q. Fan, and S.H. Guo, *Chem. Min. Process.* 49, 25 (2020).
10. M.A. Kanaparthi, and S. Dhaniyala, *J. Aerosol Sci.* 169, 106133 <https://doi.org/10.1016/j.jaerosci.2022.106133> (2023).
11. M. Kaur, A. Pandey, R. Yadav, S. Verma, and S. Husale, *Mater. Today Commun.* <https://doi.org/10.1016/j.mtcomm.2023.105741> (2023).
12. J. Uzuhashi, T. Ohkubo, and K. Hono, *Ultramicroscopy* 247, 113704 <https://doi.org/10.1016/j.ultramic.2023.113704> (2023).
13. S. Wang, R. Li, Y. Wu, and W. Wang, *Sci. Total. Environ.* <https://doi.org/10.1016/j.scitotenv.2023.162558> (2023).
14. J. Pszonka, B. Schulz, and D. Sala, *Mar. Pet. Geol.* 129, 105109 <https://doi.org/10.1016/j.marpetgeo.2021.105109> (2021).
15. K. Laakso, M. Middleton, T. Heinig, R. Bärns, and P. Lintinen, *Int. J. Appl. Earth Obs. Geoinf.* 69, 1 <https://doi.org/10.1016/j.jag.2018.02.018> (2018).
16. O. Celep, E.Y. Yazici, P. Altinkaya, and H. Deveci, *Hydrometallurgy* 189, 105106 <https://doi.org/10.1016/j.hydromet.2019.105106> (2019).
17. E. Baştürkücü, C. Şavran, A.E. Yüce, and S. Timur, *Miner. Eng.* 186, 107733 <https://doi.org/10.1016/j.mineng.2022.107733> (2022).
18. Z. Xu, Y. Li, S. Liu, L. Cai, and L. Yang, *Procedia Eng.* 102, 278 <https://doi.org/10.1016/j.proeng.2015.01.144> (2015).
19. Y. Fu, Z. Li, A. Zhou, S. Xiong, and C. Yang, *Fuel (Guildford)*. 258, 116136 <https://doi.org/10.1016/j.fuel.2019.116136> (2019).
20. P. Zhang, L. Ou, L. Zeng, W. Zhou, and H. Fu, *Powder Technol.* 343, 586 <https://doi.org/10.1016/j.powtec.2018.11.085> (2019).
21. C. Xu, C. Zhong, R. Lyu, Y. Ruan, Z. Zhang, and R.A. Chi, *J. Rare Earths* 37, 334 <https://doi.org/10.1016/j.jre.2018.06.008> (2019).
22. X. Xiao, G. Zhang, Q. Feng, S. Xiao, L. Huang, X. Zhao, and Z. Li, *Miner. Eng.* 34, 63 <https://doi.org/10.1016/j.mineng.2012.04.004> (2012).
23. M. Abdollahi, A. Bahrami, M.S. Mirmohammadi, F. Kazemi, A. Danesh, and Y. Ghorbani, *Miner. Eng.* 157, 106557 <https://doi.org/10.1016/j.mineng.2020.106557> (2020).
24. J. Yang. Study on mineral liberation characteristics and flotation behaviour of low and medium grade phosphate ores. 2022.
25. L.G. Wen, Q. Fu, M.X. Jia, and Q. Wang, *Nonferrous Metal Eng.* 12, 76 (2022).
26. L.G. Wen, M.X. Jia, Q. Wang. A new technique of automatic mineralogy based on scanning electron microscope - BPMA and its application prospect. Nonferrous Metals (Mineral Processing Section). 12-23 (2021).
27. L.G. Wen, M.X. Jia, and Q. Wang, *China Coal Geol.* 31, 8 (2019).
28. T. Ueda, T. Oki, and S. Koyanaka, *Miner. Eng.* 98, 204 <https://doi.org/10.1016/j.mineng.2016.08.026> (2016).
29. T. Ueda, T. Oki, and S. Koyanaka, *Miner. Eng.* 119, 156 <https://doi.org/10.1016/j.mineng.2018.01.034> (2018).
30. T. Ueda, T. Oki, and S. Koyanaka, *Adv. Powder Technol.* 27, 1828 <https://doi.org/10.1016/j.apt.2016.06.016> (2016).
31. T. Ueda, T. Oki, and S. Koyanaka, *Adv. Powder Technol.* 28, 1391 <https://doi.org/10.1016/j.apt.2017.03.007> (2017).

Publisher's Note Springer Nature remains neutral with regard to jurisdictional claims in published maps and institutional affiliations.

Springer Nature or its licensor (e.g. a society or other partner) holds exclusive rights to this article under a publishing agreement with the author(s) or other rightsholder(s); author self-archiving of the accepted manuscript version of this article is solely governed by the terms of such publishing agreement and applicable law.